Semiclassical investigation of Coulomb focusing effects in atomic above-threshold ionization with elliptically polarized laser fields*

Chuan-Liang Wang(王传亮)[1], Li-Xin Xia(夏立新)[1], Hong-Bin Yao(姚洪斌)[2], and Wen-Liang Li(李文亮)[2,†]

[1] *School of Physics and Electrical Engineering, Kashgar University, Kashgar* 844006, *China*

[2] *Department of Physics, Xinjiang Institute of Engineering, Urumqi* 830091, *China*

(Received 13 November 2016; revised manuscript received 22 January 2017; published online 10 March 2017)

We investigate atomic above-threshold ionization in elliptically polarized strong laser fields with a semiclassical approach. With increasing laser intensity, the Coulomb focusing (CF) effects are found to become stronger in both parallel and perpendicular directions with respect to the polarization plane. The dependence of CF effects on tunnel exit, initial transverse momentum distribution and laser electric field is analyzed. It was revealed that the effects of tunnel exit are most prominent with variation of the laser intensity, and the other two factors both play non-negligible roles. Our results provide a deeper insight to the recent experiments of Coulomb asymmetry [Shafir D, *et al.*, 2013 *Phys. Rev. Lett.* **111** 023005 and Li M, *et al.*, 2013 *Phys. Rev. Lett.* **111** 023006].

Keywords: above-threshold ionization, Coulomb focusing effect, semiclassical method, elliptically polarized laser fields

PACS: 32.80.Fb, 31.15.xg, 34.80.Dp **DOI:** 10.1088/1674-1056/26/4/043201

1. Introduction

When exposed to an ultrashort strong laser pulse, an atom or a molecule may absorb more photons than necessary for ionization. This highly nonlinear phenomenon is termed as above-threshold ionization (ATI), and the related researches have greatly contributed to our understanding of strong-field atomic and molecular dynamics.[1–3]

It was commonly accepted that for the high-intensity and long-wavelength limit, ATI process can be understood within the simpleman's model,[4] in which the motion of the liberated electron is governed by the laser electric field. This model has successfully explained the general structure of photoelectron spectra, i.e., an exponential dropoff in ionization yield up to an energy of $\sim 2U_{\rm p}$ ($U_{\rm p} = E^2/4\omega^2$, is the ponderomotive energy of the laser field), and a plateau extending to around $10U_{\rm p}$, followed by a cutoff.[5–7]

Recently, further investigations reveal that the Coulomb potential of the parent ion must be taken into account for the peculiar structures. The semiclassical analysis indicates that the dip at zero momentum of photoelectron distribution along the laser polarization direction is attributed to the Coulomb potential of the parent ion.[8,9] Later, more detailed investigations on the low-energy-structure in photoelectron spectra of atoms and molecules subjected to the mid-inferred lasers clarify the Coulomb focusing of the parent ion.[10–12] Then, the very-low-energy-structure is also found to be connected with the Coulomb potential.[13] And recently, further experiments show that the CF effects can even be more easily identified for elliptical polarization.[14,15]

Notice that in the aforementioned two experiments,[14,15] atomic strong field ionization is investigated in full three dimensions using the COLd Target Recoil Ion Momentum Spectrometer (COLTRIMS) and elliptically polarized laser fields. The CF effects are distinguished in both parallel and perpendicular directions with respect to the polarization plane. The investigations reveal the dependence of CF on the initial transverse momentum distribution, electron orbits and tunnel exit. We find that all these factors are related to laser intensity, which can be easily controlled manually.

In this paper, the atomic above-threshold ionization in elliptically polarized laser field is investigated with a semiclassical method. With increasing laser intensity, the CF effects are found to be stronger both in the polarization plane and in the perpendicular direction. The contributions of tunnel exit, transverse momentum distribution and laser electric field are explored.

2. Theoretical methods

In this paper, a semiclassical model is adopted to calculate the photoelectron spectra of atomic hydrogen. The semiclassical method retains the advantages of both quantum tunneling and classical trajectory. It requires moderate computational resources and can be easily implemented with various physical effects (such as Coulomb potential, tunnel exit, ...).[9,11–13,15–19] However, in this approach the effects of quantum interference and atomic structure are excluded. Fortunately, theses effects are expected to be insignificant in our study.

*Project supported by the National Natural Science Foundation of China (Grant Nos. 11547218, 11564020, and 11504314).

†Corresponding author. E-mail: wenliangli@vip.126.com

© 2017 Chinese Physical Society and IOP Publishing Ltd

In the semiclassical method, the bounded electron is assumed to ionize via tunneling through the barrier formed by the Coulomb potential and the quasi-static electric field.[20] Thereafter, the motion of the freed electron is completely determined by the classical Newtonian equation (The atomic unit a.u. is used throughout unless otherwise indicated.)

$$\frac{\mathrm{d}^2\boldsymbol{r}}{\mathrm{d}t^2} = -\boldsymbol{E}(t) - \nabla\frac{1}{r}, \tag{1}$$

where $\boldsymbol{E}(t) = E_0 f(t)(\cos\omega t\cdot\boldsymbol{e}_z + \varepsilon\cdot\sin\omega t\cdot\boldsymbol{e}_x)$ is the elliptically polarized laser field, with the envelope

$$f(t) = \begin{cases} 1, & t \leqslant 10T, \\ \cos^2\dfrac{(t-10T)\pi}{6T}, & 10T < t \leqslant 13T, \\ 0, & t \geqslant 13T, \end{cases} \tag{2}$$

where T is the optical period, ω is the laser frequency (here $\omega = 0.057$, corresponding to a wavelength of 800 nm).

The initial conditions, i.e., positions and momentums, of the ionized electrons are obtained from the tunneling ionization theory. For a hydrogen-like atom with ionization energy I_p, the Schrödinger equation in a uniform field E and parabolic coordinates can be reformulated as[16]

$$\frac{\mathrm{d}^2\Phi}{\mathrm{d}\eta^2} + \left(\frac{I_\mathrm{p}}{2} + \frac{1}{2\eta} + \frac{1}{4\eta^2} + \frac{E\eta}{4}\right)\Phi = 0. \tag{3}$$

Physically, equation (3) describes an electron tunneling through a one-dimensional effective potential

$$U(\eta) = -\frac{1}{4\eta} - \frac{1}{8\eta^2} - \frac{1}{8}E\cdot\eta$$

with the binding energy $K = -I_\mathrm{p}/4$. The outer turning point of the potential, i.e., the tunnel exit point) can be determined by $U(\eta_0) = K$. Then the initial position (obtained in the parabolic coordinates) can be projected into the instantaneous electric coordinates ($x' = 0$, $y' = 0$, $z' = -1/2\eta_0$) and finally into the laboratory coordinates. For the initial momentum of the tunneled electron in the instantaneous electric coordinates, the longitudinal component at is assumed to be zero, while a non-zero component perpendicular to the instantaneous electric field is introduced according to ADK theory.[21] The weight of each trajectory is evaluated by $\boldsymbol{\omega}(t_0, p_0) = \omega(0)\overline{\omega(1)}$, where[22]

$$\omega(0) = \frac{4(2I_\mathrm{p})^2}{|E(t)|}\exp\left[-\frac{2(2I_\mathrm{p})^{3/2}}{3|E(t)|}\right], \tag{4}$$

$$\overline{\omega(1)} = \frac{(2I_\mathrm{p})^{1/2}}{|E(t)|\pi}\exp\left(-\frac{p_0^2(2I_\mathrm{p})^{1/2}}{|E(t)|}\right). \tag{5}$$

In our calculations, 4×10^7 initial samples are randomly distributed in the parameter space. The evolution of the ionized electron is traced until the end of the laser field and the electron momentum is obtained then.

3. Results and discussions

In Figs. 1(a)–1(e), we present the photoelectron momentum spectra of atomic hydrogen at laser intensities between 1.0×10^{14} W/cm^2 and 2.0×10^{14} W/cm^2 for ellipticity $\varepsilon = 0.3$. The semiclassical results are in reasonable agreement with the recent experiments.[14,15] The electrons are concentrated in two lobes, which get larger with increasing laser intensity as expected.

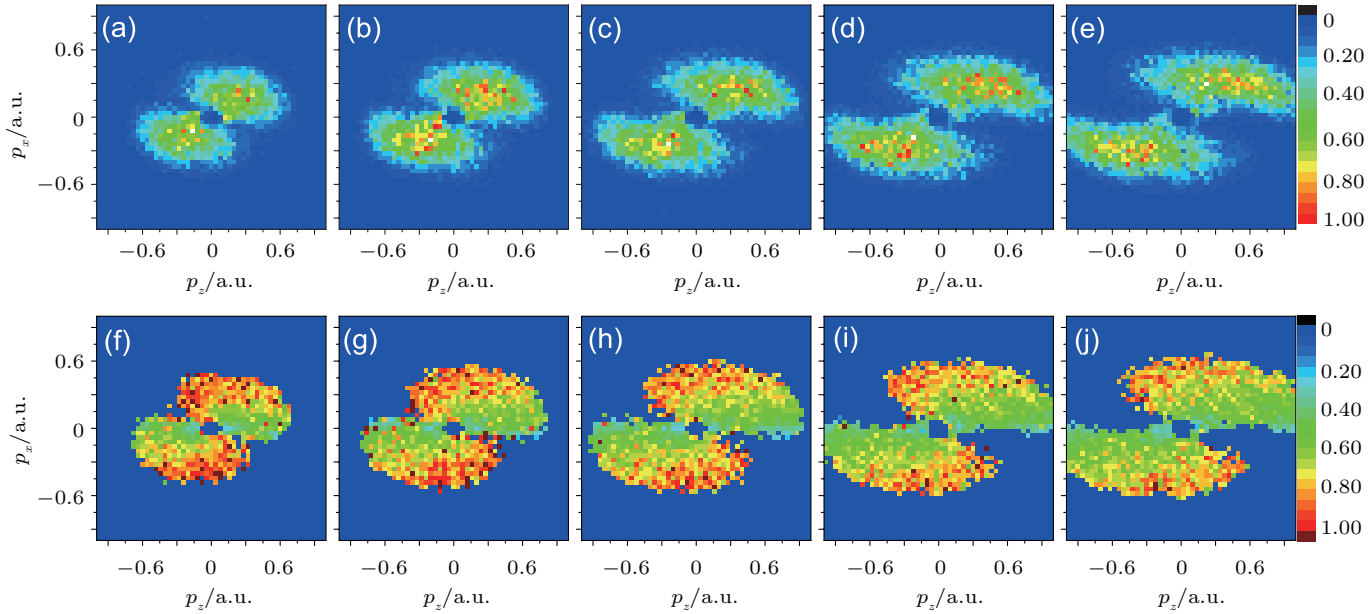


Fig. 1. (color online) Photoelectron momentum distributions of hydrogen atom for different intensities of (a) 1.0×10^{14} W/cm^2, (b) 1.25×10^{14} W/cm^2, (c) 1.5×10^{14} W/cm^2, and (d) 1.75×10^{14} W/cm^2, and (e) 2.0×10^{14} W/cm^2. The ellipticity $\varepsilon = 0.3$. All the data are normalized to unity. Panels (f)–(j) are the ratios between $\sqrt{\langle p_{\mathrm{yf}}^2\rangle}$ and $\sqrt{\langle p_{\mathrm{yi}}^2\rangle}$ for each bin in panels (a)–(e). For details, see the text.

We analyze the momentum distribution in direction perpendicular to the polarization plane (y axis, which is free of electric field) as Ref. [14]. We work out the ratios between the root-mean-square (RMS) of the final momentum $\sqrt{\langle p_{\rm yf}^2\rangle}$ and the RMS of the initial momentum $\sqrt{\langle p_{\rm yi}^2\rangle}$ for each point in the polarization plane. According to ADK theory, the initial transverse momentum distribution is gaussian, with RMS $\sqrt{|E(t)|/(8I_{\rm P})^{1/2}}$.[21] Considering that ionization mainly occurs around the field maximum, the initial RMS $\sqrt{\langle p_{\rm yi}^2\rangle}$ is approximated by $\sqrt{E_0/(8I_{\rm P})^{1/2}}$. After the evolution in the combined field of strong laser pulse and Coulomb potential, the electron distribution should be narrower. As we can see in Figs. 1(f)–1(j), the calculated ratios are generally smaller than unity, and well reproduce the experimental features.[14,15] Regions of smaller ratios and larger ratios in each lobes can clearly be distinguished, which are mainly from the contribution of rescattered electrons and direct electrons respectively.

In order to visualize the effects of laser intensity, we exhibit in Fig. 2(a) the ratios between $\sqrt{\langle p_{\rm yf}^2\rangle}$ and $\sqrt{\langle p_{\rm yi}^2\rangle}$ for all ionized electrons. As we can see, the ratios decrease almost linearly with increasing intensity. This feature indicates that CF effects play a more important role for higher laser intensity. If this is the case, the angular distribution in the polarization plane would also show the same tendency. As we can see in Fig. 2(b), the angular distribution lacks the fourfold symmetry predicted by the simpleman's model (named as Coulomb asymmetry)[23] and the electron emission peaks at about 30° and 210°. With increasing laser intensity, the angular distribution gets narrower, which indicates stronger Coulomb asymmetry. This intensity-dependence is less pronounced as the case in the y axis, probably due to the influence of the laser electric field.

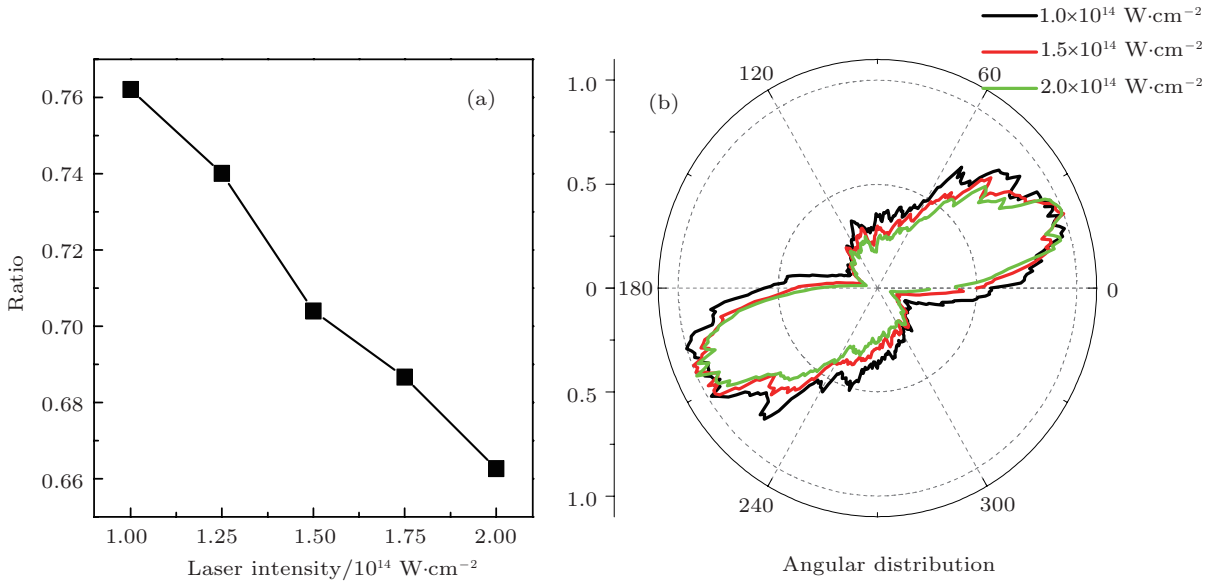


Fig. 2. (color online) (a) The ratios between $\sqrt{\langle p_{\rm yf}^2\rangle}$ and $\sqrt{\langle p_{\rm yi}^2\rangle}$ for all ionized electrons. (b) The angular distribution of ionized electrons in the polarization plane. The laser intensities range from 1.0×10^{14} W/cm^2 to 2.0×10^{14} W/cm^2 and the ellipticity $\varepsilon = 0.3$.

Our further investigations show that the Coulomb focusing effects get stronger with increasing laser intensity for ellipticity $\varepsilon < 0.5$. For larger ellipticity, the recollision plays little role in the atomic ionization, and therefore the effect of the Coulomb potential is reduced and almost independent of the laser intensity.

Then, the question is why the Coulomb focusing effects become stronger for higher laser intensity? According to the tunnelling ionization theory, the tunnel exit and the transverse momentum distribution will change with the electric field strength.[16,21] For a higher laser intensity, the tunnel exit point is closer to the parent ion, and the transverse momentum distribution becomes wider. A shorter distance from the tunnel exit point to the parent ion will undoubtedly lead to a stronger Coulomb focusing. For the initial momentum distribution, Shafir *et al.* argued that the wider transverse distribution would result in a larger probability that an electron returns to the vicinity of its parent ion, and therefore may enhance the Coulomb focusing effects.[14] However, on the other hand, a larger initial momentum distribution also means that electrons leave the parent ion faster, which translates to less influence of the Coulomb potential. Thus, the effect of the initial momentum distribution may be intricate as the case in the high-order above-threshold ionization.[17] Thanks to the semiclassical method, we can examine each factor separately.[18,19]

In the following investigation, we will explore the effect of the tunneling exit point by changing its position. For a laser intensity of 1.5×10^{14} W/cm^2, we shift the tunneling exit point η_0 by up to 30% (the plus sign '+' means moving away from the parent ion, and the minus sign '–' means

drawing closer). As we can see in Figs. 3(a) and 3(b), as the tunneling exit point draws away from the parent ion, the ratios increase dramatically and the angular distribution in the polarization plane exhibits much less Coulomb asymmetry. Both of these cases indicate stronger Coulomb focusing effects for a smaller tunneling exit point. This intuitive picture has been addressed in the previous investigations[15] and attoclock experiments.[24]

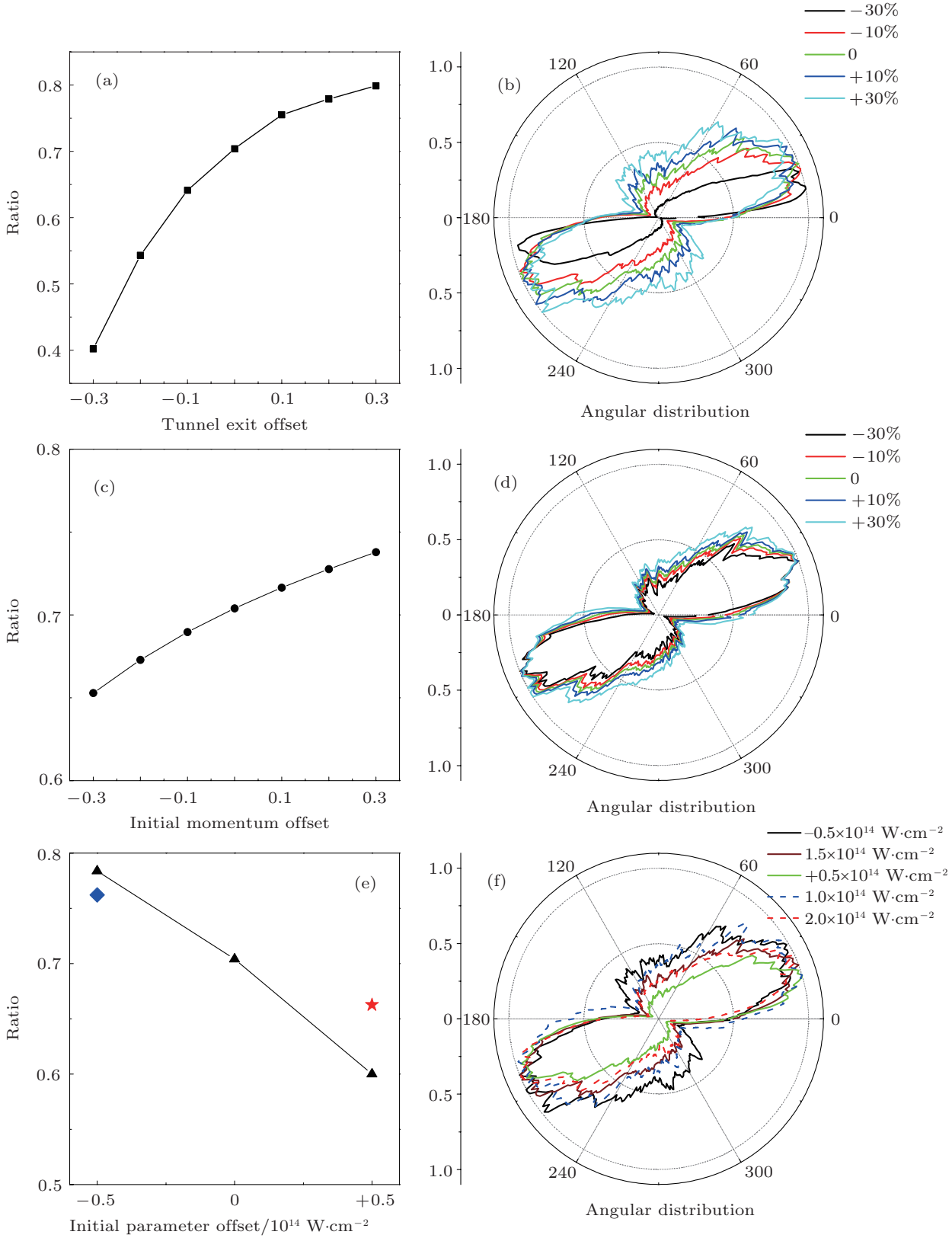


Fig. 3. (color online) (a) The ratios between $\sqrt{\langle p_{y,f}^2 \rangle}$ and $\sqrt{\langle p_{yi}^2 \rangle}$ and (b) the angular distribution in the polarization plane for different tunnel exit point offsets. (c) The ratios and (d) the angular distribution for different initial momentum distribution offsets. (e) The ratios and (f) the angular distribution for different initial parameter offsets. The laser intensity is 1.5×10^{14} W/cm^2 and the ellipticity $\varepsilon = 0.3$. The blue diamond and the red star in panel (e) are the ratios for laser intensity 1.0×10^{14} W/cm^2 and 2.0×10^{14} W/cm^2, respectively.

We further investigate electron emission with the altered initial momentum distribution. For the laser intensity of 1.5×10^{14} W/cm^2, we also change the transverse momentum distribution by up to 30%. As we can see in Fig. 3(c), the ratios increase with enlarging the width of the transverse momentum distribution, which suggests less CF effects for wider transverse momentum distribution. This feature is contradict with the predication of Shafir *et al.*[14] Also, the change of the angular distribution with the transverse momentum distribution offset [in Fig. 3(d)] shows the same tendency. Note that the effect of the initial transverse momentum distribution is far less than that of the tunnel exit point. Meanwhile, the CF effect is insensitive to the errors of the initial transverse momentum distribution. Even if the initial transverse momentum distribution has a deviation of 15%,[25] the error of the ratios between $\sqrt{\langle p_{\rm yf}^2\rangle}$ and $\sqrt{\langle p_{\rm yi}^2\rangle}$ is estimated to be less than 3%, and the main result in the article remains unchanged.

Furthermore, for an intensity of 1.5×10^{14} W/cm^2, we adopt the initial parameters, i.e., both tunnel exit point and transverse momentum distribution, for an intensity of 1.0×10^{14} W/cm^2 (named as initial parameter offset -0.5×10^{14} W/cm^2) and 2.0×10^{14} W/cm^2 (named as initial parameter offset $+0.5\times10^{14}$ W/cm^2), respectively. For the former, the tunnel exit point is about 0.25 times farther from the parent ion, and the width of the initial transverse momentum reduces by approximately 10%; for the latter, the tunnel exit point reduces to about 0.85 times of the original one, and the width of the transverse momentum enlarges by approximately 7%. As we can see in Figs. 3(e) and 3(f), for the positive initial parameter offset, the ratio gets smaller and the angular distribution gets narrower. On the contrary, the ratio becomes larger and the angular distribution gets wider for the negative initial parameter offset. This indicates that the effect of the tunnel exit surpasses that of the transverse distribution when increasing laser intensity.

Moreover, we find that for the initial parameter offset -0.5×10^{14} W/cm^2, the ratio between $\sqrt{\langle p_{\rm yf}^2\rangle}$ and $\sqrt{\langle p_{\rm yi}^2\rangle}$ is larger than that for the intensity of 1.0×10^{14} W/cm^2 [the blue diamond in Fig. 3(e)], and the main emission angle in the polarization plane shifts anticlockwise compared with the case for 1.0×10^{14} W/cm^2 [the dashed blue line in Fig. 3(f)]. On the contrary, for the initial parameter offset $+0.5\times10^{14}$ W/cm^2, the ratio is smaller than that for 2.0×10^{14} W/cm^2 [the red star in Fig. 3(e)], and the main emission angle shifts clockwise compared with that for 2.0×10^{14} W/cm^2 [the dashed red line in Fig. 3(f)]. These facts indicate that besides the initial parameters, the driving laser field also plays significant role in Coulomb focusing effects. For an ionized electron, its motion is governed by the combined forces of the laser field and the Coulomb field, which virtually compete with each other.[26] A larger momentum, i.e., kinetic energy, obtained from the laser field means relatively smaller distortion by the Coulomb potential, and *vice versa*. Therefore, for the initial parameter offset -0.5×10^{14} W/cm^2, the ionized electrons evolving in the laser field of 1.5×10^{14} W/cm^2 will obtain more momentum comparing with the case of 1.0×10^{14} W/cm^2, and will be less focused by the Coulomb potential. For the initial parameter offset $+0.5\times10^{14}$ W/cm^2, the ionized electrons acquire less momentum than that for 2.0×10^{14} W/cm^2, and will be more strongly focused by the parent ion.

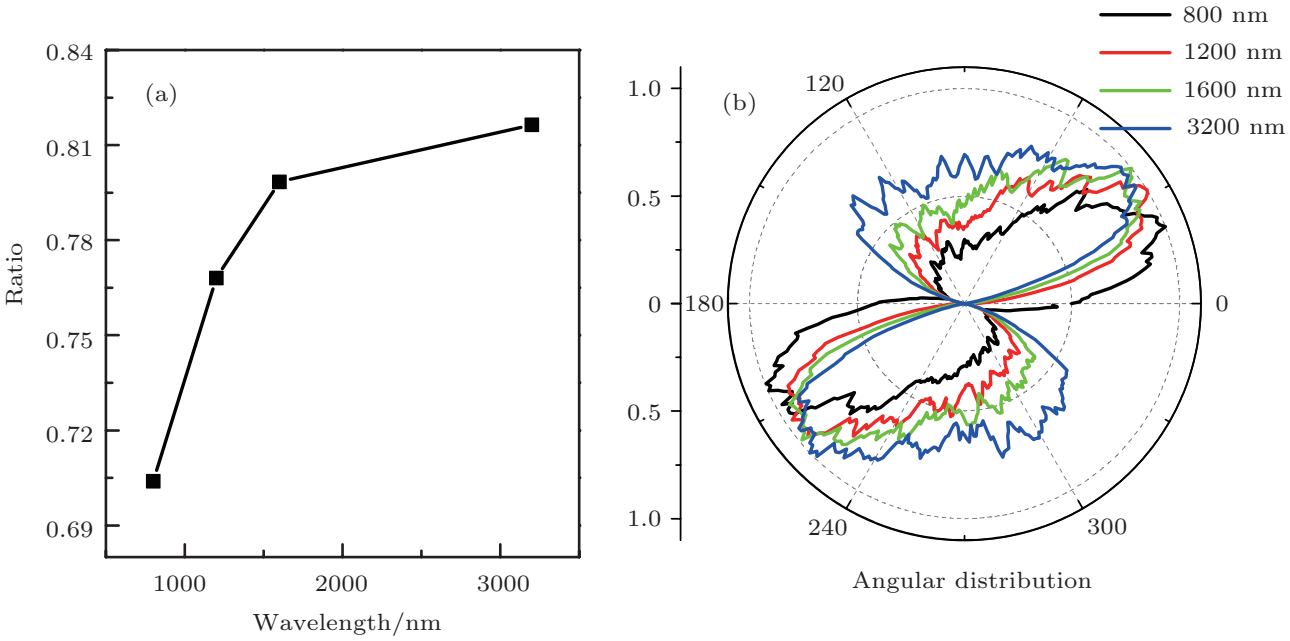


Fig. 4. (color online) (a) The ratios between $\sqrt{\langle p_{\rm yf}^2\rangle}$ and $\sqrt{\langle p_{\rm yi}^2\rangle}$, and (b) the angular distribution in the polarization plane for wavelength ranging from 800 nm to 3200 nm. The laser intensity is 1.5×10^{14} W/cm^2 and the ellipticity $\varepsilon=0.3$.

The effect of electric field can be more explicitly verified by changing the wavelength of the driving laser field. According to the quasi-static tunneling picture,[16,21] the initial conditions (the tunnel exit point and the transverse momentum distribution) are invariant to the wavelength. On the other hand, the electron's drift momentum is proportional to E_0/ω.[3] With increase of the wavelength, the electric field would show more pronounced impact on the ionization dynamics, whereas the Coulomb potential would show relatively less influences. As we can see in Figs. 4(a) and 4(b), with the increasing wavelength, the ratio between $\sqrt{\langle p_{\rm yf}^2\rangle}$ and $\sqrt{\langle p_{\rm yi}^2\rangle}$ increases dramatically, and the angular distribution becomes wider and shifts anticlockwise distinctly. Both features indicate smaller CF effects for longer wavelength. Considering the great importance of the electron recollision in the Coulomb focusing, the effect of the laser wavelength would be more pronounced for the case of the linear polarization.[27] Parenthetically, our results indicate that the laser-induced electron diffraction or the self-imaging of an atom or a molecule by its own rescattered electrons would suffer less deviation from the Coulomb potential for longer wavelength.[28,29]

4. Conclusion

In conclusion, we have investigated the above-threshold ionization of the hydrogen atom in elliptically polarized laser fields with the semiclassical method. With the increasing intensity, the ratios between the RMS of the final momentum $\sqrt{\langle p_{\rm yf}^2\rangle}$ and that of the initial momentum $\sqrt{\langle p_{\rm yi}^2\rangle}$ decrease, and the angular distribution gets narrower. These both indicate that the Coulomb focusing effect gets stronger with the increasing laser intensity. The influences of the tunnel exit point, the initial transverse momentum distribution, and the laser electric field are analyzed separately. The tunnel exit point closer to the parent ion will lead to stronger CF effects, while the larger transverse distribution will result in smaller CF effects. As for the stronger laser electric field, the CF effects are relatively less significant than that for the weaker laser electric field. Our investigation indicates that the effects of the tunnel exit are most prominent with variation of the laser intensity, and the other two factors both play non-negligible roles.

Acknowledgment

We are grateful to Dr. Quan W for many useful discussions.

References

[1] Agostini P, Fabre F, Mainfray G, Petite G and Rahman N K 1979 *Phys. Rev. Lett.* **42** 1127
[2] DiMauro L F and Agostini P 1995 *Adv. At. Mol. Opt. Phys.* **35** 79
[3] Becker W, Grasbon F, Kopold R, Milosevic D B, Paulus G G and Walther H 2002 *Adv. At. Mol. Opt. Phys.* **48** 35
[4] Corkum P B, Burnett N H, and Brunel F 1989 *Phys. Rev. Lett.* **62** 1259
[5] Schafer K J, Yang B, DiMauro L F and Kulander K C 1993 *Phys. Rev. Lett.* **70** 1599
[6] Corkum P B 1993 *Phys. Rev. Lett.* **71** 1994
[7] Paulus G G, Becker W, Nicklich N and Walther H 1994 *J. Phys. B: At. Mol. Opt. Phys.* **27** L703
[8] Moshammer R, Ullrich J, Feuerstein B, Fischer D, Dorn A, Schroter C, Lopez-urrutia J R C and Hoehr C 2003 *Phys. Rev. Lett.* **91** 113003
[9] Chen J and Nam C H 2002 *Phys. Rev. A* **66** 053415
[10] Blaga C I, Catoire F, Colosimo P, Paulus G G, Muller H G, Agostini P and DiMauro L F 2009 *Nat. Phys.* **5** 335
[11] Quan W, Lin Z Z, Wu M Y, Kang H P, Liu H P, Liu X J, Chen J, Liu J, He X T, Chen S G, Xiong H, Guo L, Xu H, Fu Y X, Cheng Y and Xu Z Z 2009 *Phys. Rev. Lett.* **103** 093001
[12] Lin Z Z, Wu M Y, Quan W, Liu X J, Chen J and Cheng Y 2014 *Chin. Phys. B* **23** 023201
[13] Wu C Y, Yang Y D, Liu Y Q and Gong Q H 2012 *Phys. Rev. Lett.* **109** 043001
[14] Shafir D, Soifer H, Vozzi C, Johnson A S, Hartung A, Dube Z, Villeneuve D M, Corkum P B, Dudovich N and Staudte A 2013 *Phys. Rev. Lett.* **111** 023005
[15] Li M, Liu Y Q, Ning Q C, Fu L B, Liu J, Deng Y K, Wu C Y, Peng L Y and Gong Q H 2013 *Phys. Rev. Lett.* **111** 023006
[16] Hu B, Liu J and Chen S G 1997 *Phys. Lett. A* **236** 533
[17] Yuan J, Li M, Sun X, Gong Q and Liu Y 2014 *J. Phys. B: At. Mol. Opt. Phys.* **47** 015003
[18] Liu C and Hatsagortsyan K Z 2010 *Phys. Rev. Lett.* **105** 113003
[19] Hao X L, Li W D, Liu J and Chen J 2012 *Chin. Phys. B* **21** 083304
[20] Landau L D and Lifshitz E M 1977 *Quantum Mechanics* (New York: Pergamon)
[21] Delone N B and Krainov V P 1991 *J. Opt. Soc. Am. B* **8** 1207
[22] Ammosov M V, Delone N B and Krainov V P 1986 *Zh. Eksp. Teor. Fiz.* **91** 2008 [1986 *Sov. Phys. JETP* **64** 1191]
[23] Goreslavski S P, Paulus G G and Popruzhenko S V 2004 *Phys. Rev. Lett.* **93** 233002
[24] Pfeiffer A N, Cirelli C, Smolarski M, Dimitrovski D, Abu-samha M, Madsen L B and Keller U 2012 *Nat. Phys.* **8** 76
[25] Arissian L, Smeenk C, Turner F, Trallero C, Sokolov A V, Villeneuve D M, Staudte A and Corkum P B 2010 *Phys. Rev. Lett.* **105** 133002
[26] Xie X, Roither S, Gräfe S, Kartashov D, Persson E, Lemell C, Zhang L, Schöffler M S, Baltuška A, Burgdörfer J and Kitzler M 2013 *New J. Phys.* **15** 043050
[27] Comtois D, Villeneuve D M and Corkum P B 2005 *J. Phys. B: At. Mol. Opt. Phys.* **38** 1923
[28] Huismans Y, Rouzée A, Gijsbertsen A, *et al.* 2011 *Science* **331** 61
[29] Blaga C I, Xu J, DiChiara A D, Sistrunk E, Zhang K, Agostini P, Miller T A, DiMauro L F and Lin C D 2012 *Nature* **483** 194